

## ASSESSMENT OF NIGERIAN LAUMONTITE ZEOLITE IN THE ADSORPTION OF ACID RED 27 AND BRILLIANT GREEN DYE IN SYNTHETIC WASTEWATER

Kovo A.S\*, Faridat J., Hawa Manko and Eluwa V.

Department of Chemical Engineering, Federal University of Technology, Minna

\*kovo@futminna.edu.ng, 07013377258

### ABSTRACT

*This study dwell on the removal of color of two different dye types namely Acid Red-27 (AA27) and Brilliant Green (BG) in a simulated waste dye water. An adsorption process in which the parameters were optimized with response surface methodology was adopted. Numerical optimization was determined at optimum conditions for BG and AA27, respectively and was used in carrying out a batch equilibrium studies while studying the effect of contact time, initial concentration and adsorbent dosage. The outcome of the experimentation indicate that the adsorbent dosage of the dye solution had a significant impact on adsorption. The result also showed that Freundlich isotherm fit the isotherm model for AA27, and Langmuir isotherm fit that of BG. The overall experimental data indicate a maximum removal of 96.24 % and 83.10 % was found for Brilliant Green and Acid Red 27 respectively while the maximum dye adsorption capacity of BG and AA27 was obtained at 68.02 and 3.43 mg/g, respectively. Activated Nigerian Laumontite zeolite has capability for adsorption and hence can be used for effective removal of dyes from wastewater.*

**Keywords:** Laumontite zeolite; Brilliant green dye; Acid red 27; Adsorption; Laumontite

### 1. INTRODUCTION

The production of numerous pollutants due to industrialization and modernization has negatively impacted the environment (Bushra *et al.*, 2021). The use of water by many different process industries and its attendant effects through discharges pose an enormous challenge environmentally. Brilliant green is currently used in industry worldwide for a variety of tasks, including dying paper, leather, wool, and silk. Veterinary care, dermatological products, biological stains. Acid red 27 is useful as a food dye. It is also used in cosmetics, natural and synthetic fibers, leather, paper, and phenol-formaldehyde resin. This usefulness in the mentioned processes entails they are present in the wastewater released by several process industries, including textile industry (Zafar *et al.*, 2020). The level of Water pollution beyond the threshold limit is directly related to the general effects such as gastrointestinal tract which can lead to other secondary effect including nausea, vomiting, and diarrhea, and even coughing and shortness of breath.

There are several technologies available that are used for the removal of organic contaminants. These include oxidation method (Pathania *et al.*, 2016), treatment using biotic processes (Santos and Boaventura, 2015), the use of membrane process [Lau and Ismail, 2009], coagulation/flocculation, and adsorption (Wu *et al.*, 2017). Adsorption processes are the most widely used treatment techniques for eliminating organic contaminants (Mahmoud *et al.*, 2020) because of its simplicity and effectiveness as well as economical advantage over other processes (Albadarin *et al.*, 2017). There are several adsorbents well known to possess good adsorption properties such as activated carbon, fly ash,

clay minerals and zeolites. Zeolite is an aluminosilicate material (both synthetic and natural) with a polyhedral three-dimensional structure made up of  $[\text{SiO}]^{4-}$  and

$[\text{AlO}]^{5-}$  complexes. These compounds have a specific chemistry and qualities that make it possible for them to adsorb various environmental pollutants (Alakhras *et al.*, 2020). Laumontite natural zeolites which have been studied extensively used as adsorbents was recently discovered in part of Nigeria and they are known to have good surface area, porous structure, and ion-exchange capabilities. This study is therefore aim to assess the efficacy of this new natural zeolite (NZ) sourced from Adamawa, Nigeria as an adsorbent for wastewater treatment by removing Acid Red 27 and Brilliant Green dye.

### 2. MATERIALS AND METHODS

#### 2.1. Materials

Natural laumontite zeolite (NLZ) was sourced from Ganki, Fufure LGA in Adamawa State, Nigeria. All chemical used in this work were of analytical grade.

#### 2.2. Purification and Modification of the Adsorbent material

First, 100 g of NLZ was crushed and sieved using 300  $\mu\text{m}$  mesh, this was then followed by washing of the sieved NLZ with large quantity of deionized water to remove impurities and finally dried in oven for 6 h at 110  $^{\circ}\text{C}$ . The activation of the natural zeolite was carried with the aid of NaCl. The activation process to convert LAU-NZ in Na-form was prepared according to previous procedures described in the literature (Hasan, 2023). 28.89 g of NLZ was added to 1M NaCl solution which was stirred for 20 h at 50 rpm. The material was decanted, and was washed

four times with deionized water to remove excess sodium chloride and finally dried in the oven at 110 °C for 9 h.

### 2.3. Characterization of natural Laumontite zeolite

The analysis of NLZ and activated NLZ before and after the adsorption of brilliant green and acid red 27 was carried out using by Fourier transform infrared spectroscopy (FT-IR) for it functional groups, the microstructure/morphology was performed by a scanning electron microscope (SEM), the X-ray fluorescence was used to determine a material's oxide composition, and the crystallographic structural properties was determined by X-ray powder diffraction (XRD) (Model: EMPYREAN from Netherlands) in the 2θ range of 5-70.

### 2.4 Empirical optimization design

Box-Behnken (BBD) was employed to evaluate the impact of process factors on the removal efficiency of BG AND AA27 on NLZ. The selected variables were initial concentration (40 – 200 mg/l), Contact time (30 – 240 min) and adsorbate dosage (0.05 -0.3 g). 17 experiment runs were generated using Design Expert software (Ver.13.0).

**Table 1 Independent factors and their chosen level of the experimental design**

Name	Symbol	Low	High
Contact time (min)	A	30	240
Adsorbent dosage (g)	B	0.05	0.3
Initial concentration (mg/l)	C	40	200

**Table 2 Full BBD Experimental Design Table**

	Factor 1	Factor 2	Factor 3
Runs	A: Initial concentration (mg/l)	B: Contact time (min)	C: Adsorbent dosage (g)
1	40	30	0.175
2	120	240	0.05
3	40	135	0.05
4	120	135	0.175
5	40	135	0.3
6	200	30	0.175
7	120	30	0.3
8	120	135	0.175
9	120	135	0.175
10	120	135	0.175
11	200	135	0.3
12	120	30	0.05
13	40	240	0.175
14	200	135	0.05
15	120	135	0.175
16	200	240	0.175
17	120	240	0.3

Diagnostic plots and analysis of Variance (ANOVA) were utilized in the statistical study to evaluate the statistical significance of the regression coefficient of the suggested models and optimum conditions for the adsorption process.

### 2.5 Numerical Optimization

Numerical optimizations were performed using the 'optimization' selection on Design Expert v13.0. Maximizing removal efficiency within the parameters and keeping all process variables within them were the objectives of the numerical optimization, subject to a few carefully considered constraints (Bader *et al.*, 2018; Cui *et al.*, 2019).

### 2.6 Adsorption experiment

The adsorption of BG and AA27 on activated NLZ was carried out by batch method. This was done by shaking 50 ml of a known initial dye concentration with known amount the adsorbent NLZ in 250 mL and the solution was stirred at 210 rpm according to the experimental variables obtained from the design factors as given by the BBD experimental design. The solution of the adsorbent and adsorbate were separated using a filter paper and the filtrate was tested for the absorbance using a UV-visible spectrophotometer. All samples were filtered before the residual acid red 27 and brilliant green quantity were quantified using UV spectroscopy at 519.50 nm and 624.50 nm respectively.

The amount of dye adsorbed at equilibrium  $q_e$  (mg/g) was calculated at equilibrium condition using Eq. (1):

$$Q_e = \frac{C_0 - C_e}{w} * V \quad (1)$$

Where  $C_0$  and  $C_t$  are the initial concentration and final concentration of Acid red 27 and Brilliant green in the solution (mg/L);  $V$  is the volume of Acid red 27 (L);  $W$  is the weight of adsorbent (g).

The removal efficiency was calculated using equation 2:

$$R = \frac{C_0 - C_t}{C_0} \times 100\% \quad (2)$$

Where  $C_0$  and  $C_t$  are the initial concentration and final concentration of Acid red 27 and Brilliant green in the solution (mg/L).

#### 2.6.1 Adsorption isotherms

The experimental data was analyzed using Langmuir and Freundlich isotherms, and the molecular distribution of adsorbate on the adsorbent surface was done for [Jahan *et al.*, 2023] acid red 27 and brilliant green (Zafar *et al.*, 2020; Mansour *et al.*, 2020) for their adsorption characteristic.

Equation 3 represents the linear Langmuir model:

$$\frac{C_e}{q_e} = \frac{C_e}{q_{\max}} + \frac{1}{q_{\max} K_L} \quad (3)$$

where  $q_e$  is the equilibrium adsorption, and  $q_{\max}$  is the maximum adsorption capacity (mg/g),  $C_e$  is the

equilibrium concentration (mg/L) related, and  $k_L$  is the Langmuir isotherm constant (L/mg) related to the affinity of the binding sites to the adsorbate

Equation 4 represents the linear Freundlich model:

$$\log q_e = \log K_f + \frac{1}{n} \log C_e \quad (4)$$

The parameter in equation 3 are describe as follows,  $q_e$  is the equilibrium adsorption (mg/g),  $C_e$  is the equilibrium concentration (mg/L),  $k_F$  is the Freundlich isotherm constant (mg/g), and  $1/n$  is dimensionless representing the heterogeneity of the adsorbent sites and also indicates the affinity between adsorbate and adsorbent.

### 3. RESULTS AND DISCUSSION

#### 3.1. Zeolite Analysis

The first five 2-theta peaks in the diffractogram clearly match the pattern of typical peaks for NLZ as described in the literature, which displays all of the peaks that are characteristic for Laumontite (Treacy and Higgins, 2007). The X-ray diffractograms of NLZ in (Fig.2a) show that the main diffraction peaks at 2 $\theta$  angles, major peak values for the first five 2-theta of the samples are seen at around 7.5°, 12.5°, 25.0°, and 28.5° corresponding to hkl plains of (110), (200), (-112), and (330), respectively. The SEM images of NLZ as shown in fig 2b micrograph displayed a large plate-like structure, suggesting that the silica and alumina are sliding over one another, and the SEM micrograph revealed a uniform particle size of the sample with a regular shape when compared with literature (Hosaka *et al.*, 1995).

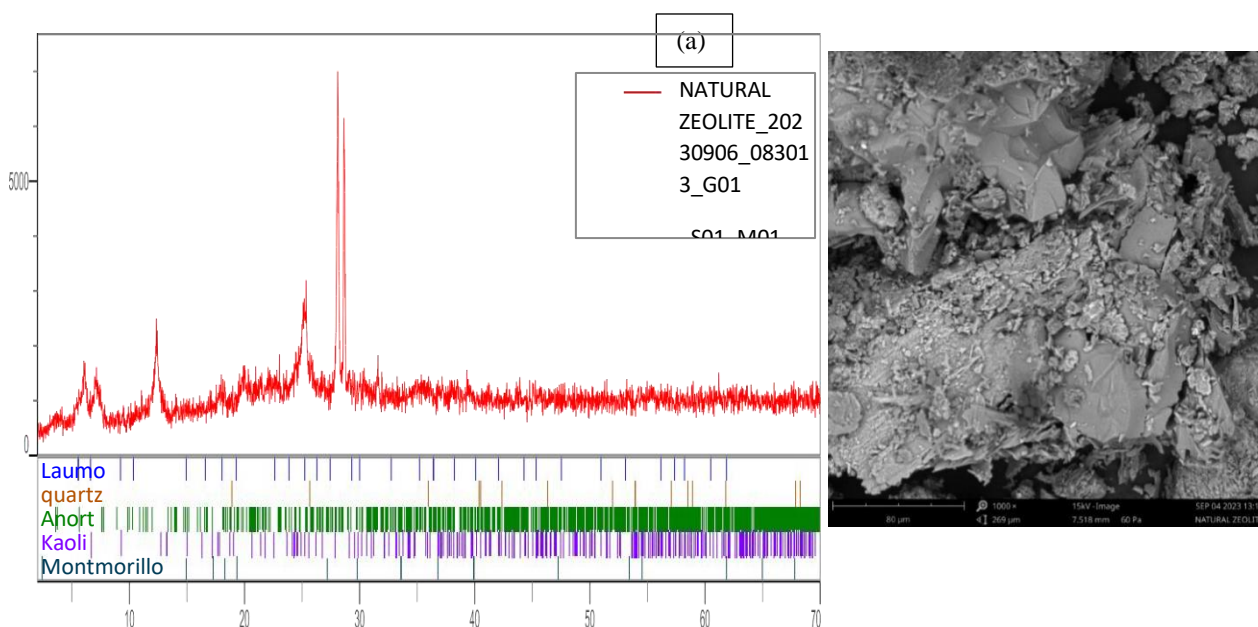


Figure 2. (a) X-ray diffractogram of LAU-NZ and (b) SEM image of LAU-NZ

The XRF analysis result as shown in Table 3 was used to determine the oxides and elemental compositions of the NLZ. The result as shown in table 3 present results from

the X-ray Fluorescence analysis clearly indicate the preponderance of various oxide composition of the natural material

Table 3 shows the oxides, elements, and percentage weight concentrations of LAU-NZ.

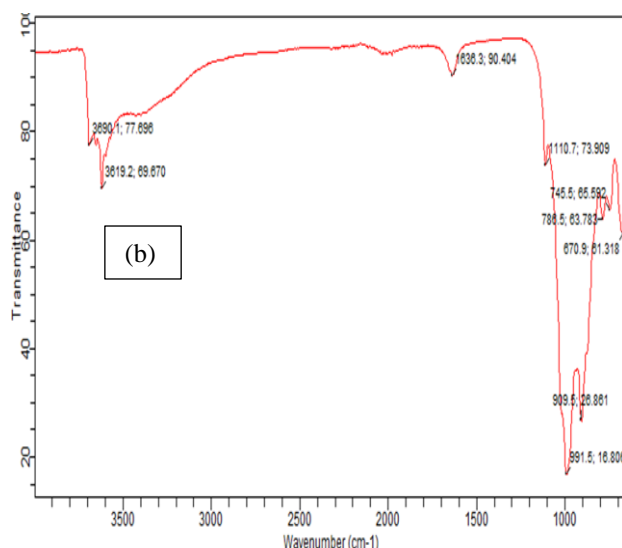
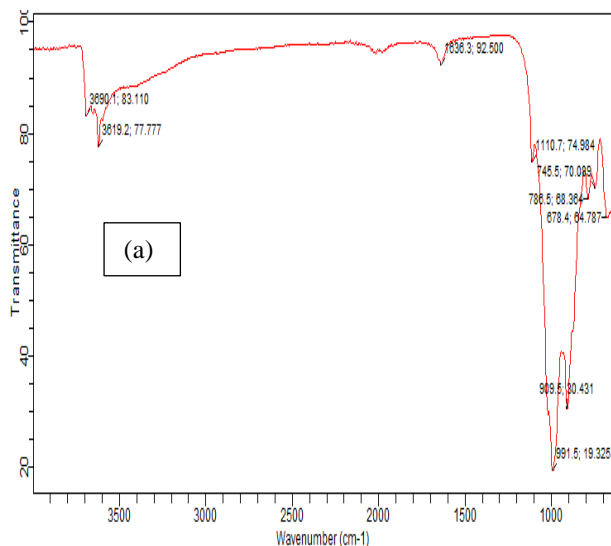
OXIDES	CONCENTRATION WT. %	ELEMENT	CONCENTRATION WT. %
SiO <sub>2</sub>	46.524	O	45.545
V <sub>2</sub> O <sub>5</sub>	0.068	Al	11.194
Cr <sub>2</sub> O <sub>3</sub>	0.150	Si	21.747
MnO	0.135	S	2.036
Fe <sub>2</sub> O <sub>3</sub>	15.170	Cl	0.487

OXIDES	CONCENTRATION WT.%	ELEMENT	CONCENTRATION WT.%
Co <sub>3</sub> O <sub>4</sub>	0.051	K	1.348
NiO	0.041	Ca	6.021
CuO	0.040	Ti	0.538
Nb <sub>2</sub> O <sub>3</sub>	0.015	V	0.038
MoO <sub>3</sub>	0.023	Cr	0.103
SO <sub>3</sub>	5.085	Mn	0.104
CaO	8.424	Fe	0.611
K <sub>2</sub> O	1.624	Co	0.037
BaO	0.073	Ni	0.032
Al <sub>2</sub> O <sub>3</sub>	21.150	Cu	0.032
Ta <sub>2</sub> O <sub>5</sub>	0.004	Zn	0.015
TiO <sub>5</sub>	0.897	Zr	0.016
ZnO	0.019	Nb	0.012
ZrO <sub>2</sub>	0.022	Ba	0.066

The sample has Si/Al ratio greater than one (1.942 as shown in Table 3). Given that the minimal Si/Al ratio should be 1 and 1.3 – 3.3. the outcome appears to be in line with Breck DW and Loewenstein's rule for aluminum in four-fold coordination respectively (Soscún *et al.*, 2001).

FTIR spectra of activated NLZ, adsorbed AA27, and adsorbed BG in Fig.3 shows the band (4000 - 2500 cm<sup>-1</sup>) is the stretching vibrations of Si-OH and Si-OH-Al, the band at (2500 - 2000 cm<sup>-1</sup>) are attributed to the bending vibrations of water molecules H-O-H, (2000 - 1500 cm<sup>-1</sup>)

is due to asymmetric stretching vibrations of (C=O), and (1500 -400 cm<sup>-1</sup>) asymmetric and symmetric stretching vibration of internal (Kumar, 2019). In Fig.3c, distinct absorption peaks at (1192.7 -1,786.5 cm<sup>-1</sup>) are attributed to the asymmetric stretching vibration of internal T-O(T) bonds and symmetric stretching vibration of internal T-O(T) bonds (Hasan, 2023) and Fig.3b, The minimal shift of the T-O bond and C=O bands after loading the dye is due to the strong intensities surface complexation of the dye substance with these functional groups.



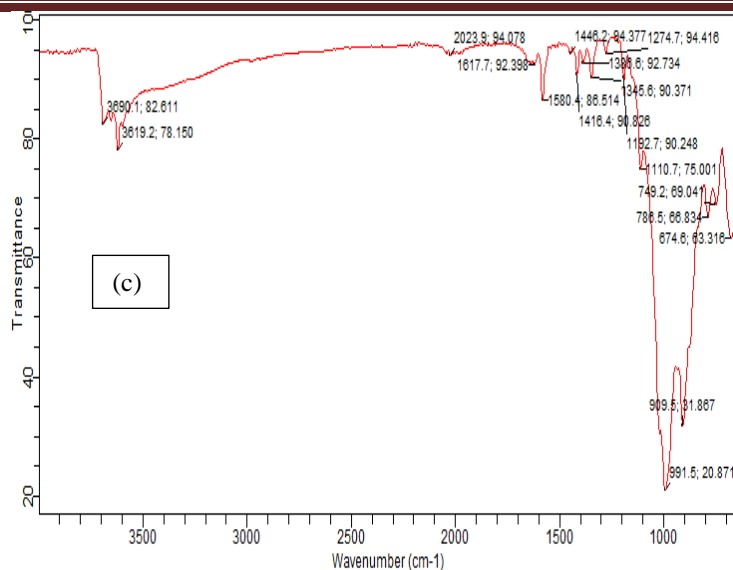


Figure 3. FTIR analysis on (a) Activated zeolite, (b) Adsorbed AA 27, and (c) Adsorbed BG

### 3.2 ANOVA and Diagnostic model

The results of the ANOVA demonstrated that the relationships between each response and the important factors were accurately reflected by the equations. According to the model, A, B, C, AB<sup>2</sup>, AC<sup>2</sup>, BC<sup>2</sup>, A<sup>2</sup>, B<sup>2</sup>, and C<sup>2</sup> were significant model terms. Additionally, lack of fit became critical because of certain systematic fluctuations that this model was unable to account for. Equations (5) and (6) of the software's model showed how the independent parameters taken into account and % removal of BG and AA27 are related.

$$\begin{aligned} \% \text{ Removal} = & +91.5231 + 4.51816 A - 0.159446 B + \\ & 0.478342 C + 0.440712 AB \\ & - 0.167962 AC + 0.795563 BC - 3.72207A^2 \\ & - 0.12296 B^2 + 0.347415 C^2 \end{aligned} \quad (5)$$

$$\begin{aligned} \% \text{ Removal} = & +99.40 + 0.9539 A - 0.0380 B + 0.1481 C \\ & - 0.2492 AB - 0.6224 AC + 0.4053 BC \\ & - 0.9194 A^2 + 0.0669 B^2 - 0.4996 C^2 \end{aligned} \quad (6)$$

An increase or decrease in response resulting from independent and interaction factors is indicated by a positive or negative sign in the equation. The adsorption yield is greatly influenced by all three of the parameters, according to the ANOVA analysis. In contrast, for both dyes, the adsorption yield is positively impacted by the dye concentration and adsorbate dosage in solution; the activated zeolite contact time has a negative impact according to the correlation coefficients

The preparation conditions and experimental results for the studied responses are shown in Table 4. Values of adsorption capacities varied between 9.50 and 184.95 mg/g for AA27 and between 6.52 and 198.78 mg/g for BG. The highest values of 184.95 and 198.78 mg/g were obtained for the activated zeolite of 0.05 g.

Table 4: Box-Behnken design actual values and experimental results responses

Run	Actual values			Qe (mg/g)		%Removal	
	Contact time (min)	Adsorbate dosage (g)	Dye Concentration (mg/g)	AA27	BG	AA27	BG
1	30	0.175	40	9.50	11.12	83.14	97.31
2	240	0.05	120	109.42	117.99	91.18	98.33
3	135	0.05	40	33.65	38.50	84.13	96.24
4	135	0.175	120	31.33	34.04	91.38	99.30
5	135	0.3	40	5.47	6.52	81.10	97.82
6	30	0.175	200	52.75	56.98	92.32	99.72
7	30	0.3	120	18.14	19.76	90.72	98.81

*Assessment of nigerian laumontite zeolite in the adsorption of acid red 27 and brilliant green dye in synthetic wastewater*

Run	Actual values			Qe (mg/g)		%Re moval	
	Contact time (min)	Adsorbate dosage (g)	Dye Concentration (mg/g)	AA27	BG	AA27	BG
8	135	0.175	120	31.52	34.10	91.92	99.47
9	135	0.175	120	31.10	34.12	90.70	99.51
10	135	0.175	120	31.30	34.08	91.29	99.39
11	135	0.3	200	30.70	33.16	92.11	99.48
12	30	0.05	120	110.04	119.23	92.70	99.36
13	240	0.175	40	9.64	11.19	84.31	97.88
14	135	0.05	200	184.95	198.78	92.48	99.39
15	135	0.175	120	31.66	34.06	92.33	99.35
16	240	0.175	200	53.04	56.74	92.81	99.30
17	240	0.3	120	18.68	19.88	93.39	99.39

**Table 5: Analysis of variance for AA27 model**

Source	Sum of Squares	df	Mean Square	F-value	p-value	
<b>Model</b>	227.60	9	25.29	52.20	< 0.0001	significant
A-Initial concentration	163.31	1	163.31	337.06	< 0.0001	
B-Adsorbate dosage	0.2034	1	0.2034	0.4198	0.5377	
C-Contact time	1.83	1	1.83	3.78	0.0930	
AB	0.7769	1	0.7769	1.60	0.2459	
AC	0.1128	1	0.1128	0.2329	0.6441	
BC	2.53	1	2.53	5.23	0.0561	
A <sup>2</sup>	58.33	1	58.33	120.39	< 0.0001	
B <sup>2</sup>	0.0637	1	0.0637	0.1314	0.7277	
C <sup>2</sup>	0.5082	1	0.5082	1.05	0.3398	
Residual	3.39	7	0.4845			
Lack of Fit	1.83	3	0.6095	1.56	0.3305	not significant
Pure Error	1.56	4	0.3908			
Cor Total	230.99	16				

**Table 6: Analysis of variance for BG model**

Source	Sum of Squares	df	Mean Square	F-value	p-value	
<b>Model</b>	14.75	9	1.64	148.95	< 0.0001	significant
A-Initial concentration	7.28	1	7.28	661.60	< 0.0001	
B-Contact time	0.0115	1	0.0115	1.05	0.3401	
C-Adsorbate dosage	0.1755	1	0.1755	15.95	0.0052	
AB	0.2484	1	0.2484	22.57	0.0021	
AC	1.55	1	1.55	140.82	< 0.0001	
BC	0.6572	1	0.6572	59.73	0.0001	
A <sup>2</sup>	3.56	1	3.56	323.48	< 0.0001	
B <sup>2</sup>	0.0189	1	0.0189	1.71	0.2319	
C <sup>2</sup>	1.05	1	1.05	95.54	< 0.0001	

<b>Residual</b>	0.0770	7	0.0110			
Lack of Fit	0.0467	3	0.0156	2.06	0.2488	not significant
Pure Error	0.0303	4	0.0076			
<b>Cor Total</b>	14.83	16				

Fig. 4, provides statistical actual and predicted values to test the significant effects of regression coefficients for the proposed models. In Fig. 4a, which showed the distribution of BG adsorption data points close to the straight line, while AA27 data in Fig. 4b deviated from the straight line. Consequently, there was a reasonable agreement between the " $R^2$ " and the " $R^2_{adj}$ ". Additionally,

" $R^2$ " was higher than " $R^2_{adj}$ ". It is evident that over 90% of these reactions are accurately anticipated by these models, suggesting that the terms taken into account in the suggested models were important enough to produce predictions that could be accepted (Tounsadi, *et al.*, 2016).

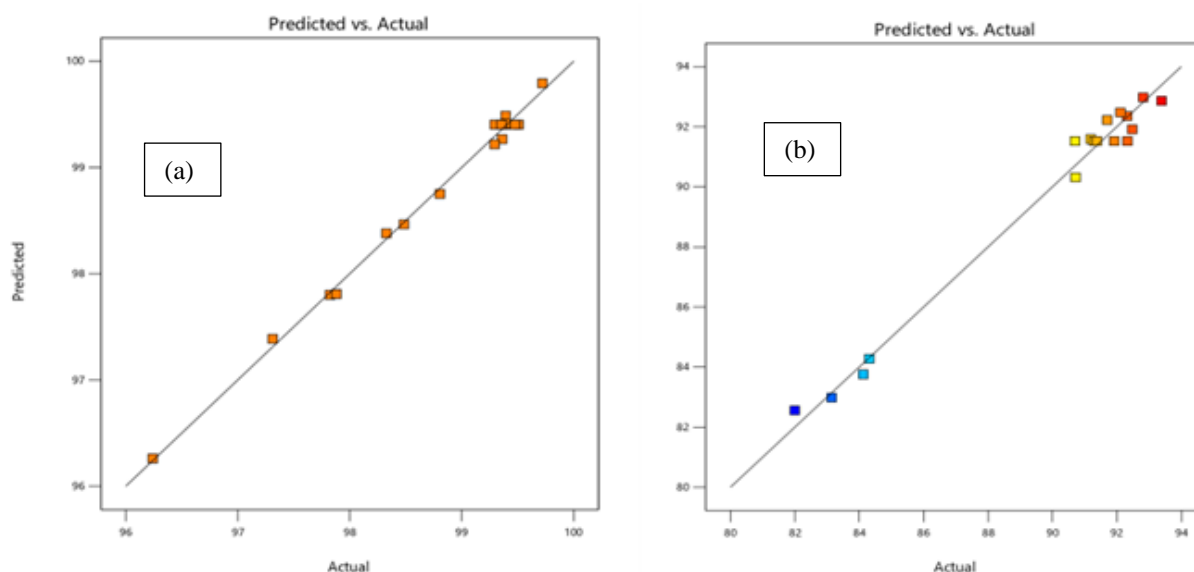


Figure 4: Predicted values vs. actual values for (a) BG, and (b) AA27

### 3.3 Numerical Optimization

Maximizing removal efficiency within the parameters and keeping all process variables within them were the objectives of the numerical optimization, subject to a few

carefully considered constraints (Bader *et al.*, 2018; Cui *et al.*, 2019). These constraints are presented in Table 7 and 8 for the dyes below.

Table 7: Factor and response constraints on the numerical optimization for BG

Name	Goal	Lower Limit	Upper Limit	Lower Weight	Upper Weight	Importance
A: Initial concentration	is in range	40	200	1	1	3
B: Contact time	is in range	30	240	1	1	3
C: Adsorbate dosage	is in range	0.05	0.3	1	1	3
Removal	maximize	96.2417	99.721	1	1	3

Table 8: Factor and response constraints on the numerical optimization for AA27

Name	Goal	Lower Limit	Upper Limit	Lower Weight	Upper Weight	Importance
A: Initial concentration	is in range	40	200	1	1	3
B: Adsorbate dosage	is in range	0.05	0.3	1	1	3
C: Contact time	is in range	30	240	1	1	3
% Removal	maximize	81.9975	93.387	1	1	3



Table 6 and 7, shows the maximum removal efficiencies were observed to be 96.24% and 81.10% for BG and AA27 dyes, respectively. The optimum condition for BG is at initial concentration of 190.428 mg/l, adsorbent dosage of 0.159 g, and contact time of 69 min and that of AA27 at initial concentration of 166.649 mg/l, adsorbent dosage of 0.274 g, and contact time of 210 min. The desirability values of these parameters which is a show of the ideal and desired values were observed to be 1.000 (unity) for the two dyes. The result indicate the acceptance of the predicted adsorption removal efficiencies and the applicationn of the model for the dyes removals .

### 3.4 Batch adsorption experiment

#### 3.4.1. Effect of initial concentration

A plot of removal efficiency of the BG dye is shown in Figure. 5a, while keeping other factors constant

(adsorbent dosage = 0.159 g, contact time = 69 min). It can be observed that the number of active sites on the surface of the adsorbent is more available at low initial dye concentrations than it is at high initial dye concentrations. The removal efficiency of BG rises proportionally with the initial concentration (Alene *et al.*, 2020). In Fig. 5b, while keeping other factors constant (adsorbent dosage = 0.274 g, contact time = 210 min), the removal efficiency of AA27 increases inversely with the initial concentration. The number of effective adsorption sites on the adsorbents exceeds the number of competent AMD molecules at lower starting concentrations. Because of this, a greater percentage of AA 27 molecules exhibit increased adsorption effectiveness when they are bound to the adsorbent surface (Rahaman *et al.*, 2022). This show that these process favors at higher concentration.

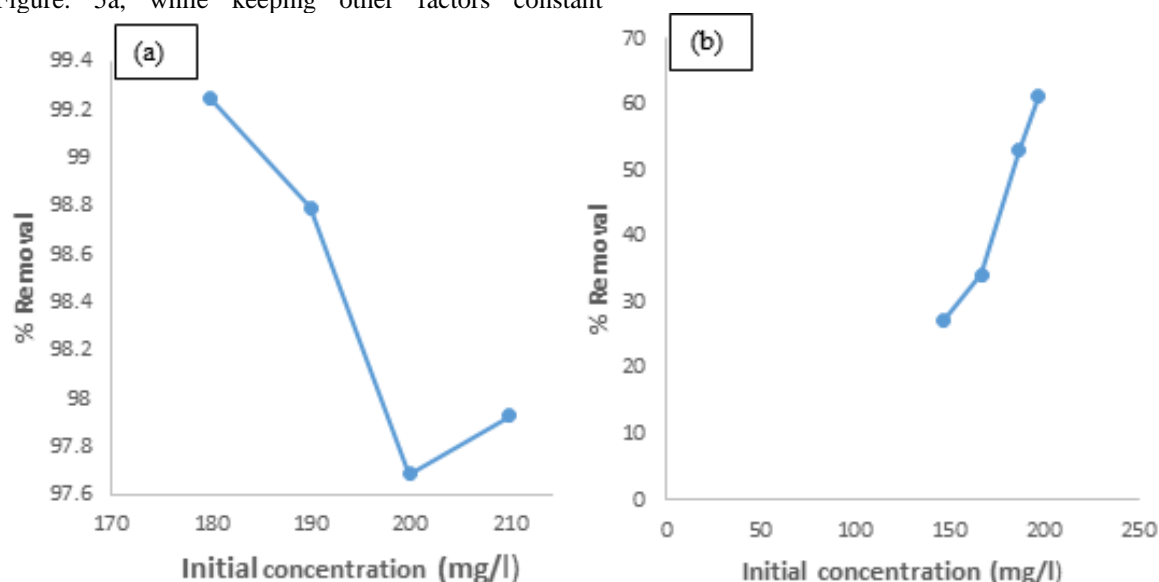


**Figure 1: Effect of initial concentration on adsorption of (a)BG dye, and (b) AA27 onto AZ**

#### 3.4.2 Effect of adsorbent dosage

The plot of removal efficiency against adsorbent dosage as presented in Figure. 6 shows that adsorbent dosage is one of the independent variables that can alter the dye removal efficiency. The study was at constant conditions of initial concentration = 190 mg/l and contact time=69 min for BG and initial concentration = 167 mg/l and contact time= 210 min for AA27, respectively. Between

the two dyes, the removal efficiency of BG is greater than that of AA27 as shown in the plot with changes in the activated zeolite dosage which is due to the amount of more adsorbent active sites and more adsorbent specific surface area become available, leading to an increase in the removal percentage of both dyes onto activated zeolite (AZ) (Alene *et al.*, 2020).



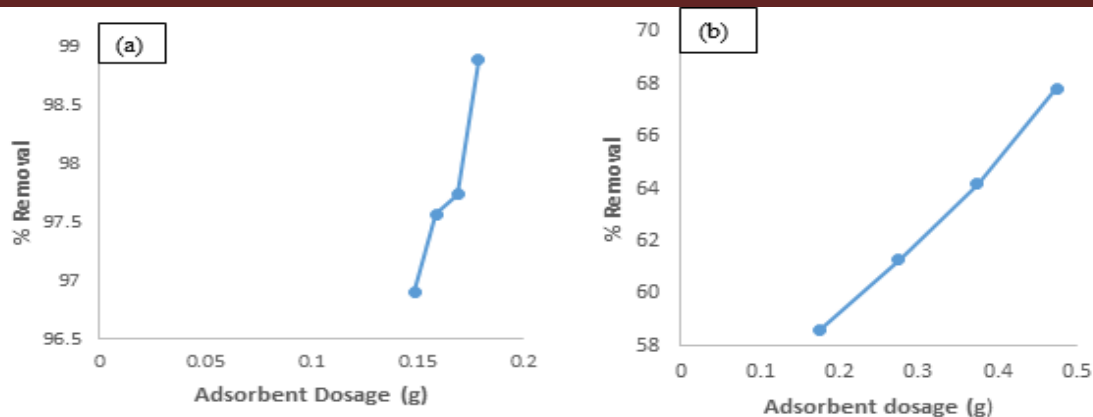


Figure 2: Effect of adsorbent dosage on adsorption of (a)BG dye, and (b)AA27 onto AZ

### 3.4.3 Effect of contact time

The effect of removal efficiency on contact time was studied at constant conditions of (Adsorbent dosage = 0.159 g and initial concentration = 190 mg/L) for BG and that of AA27 (Adsorbent dosage = 0.274 g and initial concentration = 167 mg/L) efficiencies of both dyes were affected by contact time as observed from Fig. 7. From the plot, it was noticed that the removal efficiency for the dyes increased with longer time of contact between the activated LAU-NZ and adsorbate. In Fig. 7a, It is evident that the dye's initial removal efficiency increased during

the first 59 minutes, and that this was followed by a slow removal rate until the 89-minute mark. However, as equilibrium takes longer to reach, the number of surface sites that remain will decrease and it will become more difficult to occupy these ions (Samaka, 2021) whereas, in Fig. 7b, it was observed that there was a steep increase in the amount of dye adsorbed from 210 - 230 minutes which follows by a steady increase. Due to the unavailability of the active adsorption sites on the adsorbent surface, the adsorption effectiveness falls as the contact time increases (Munagapati *et al.*, 2021).

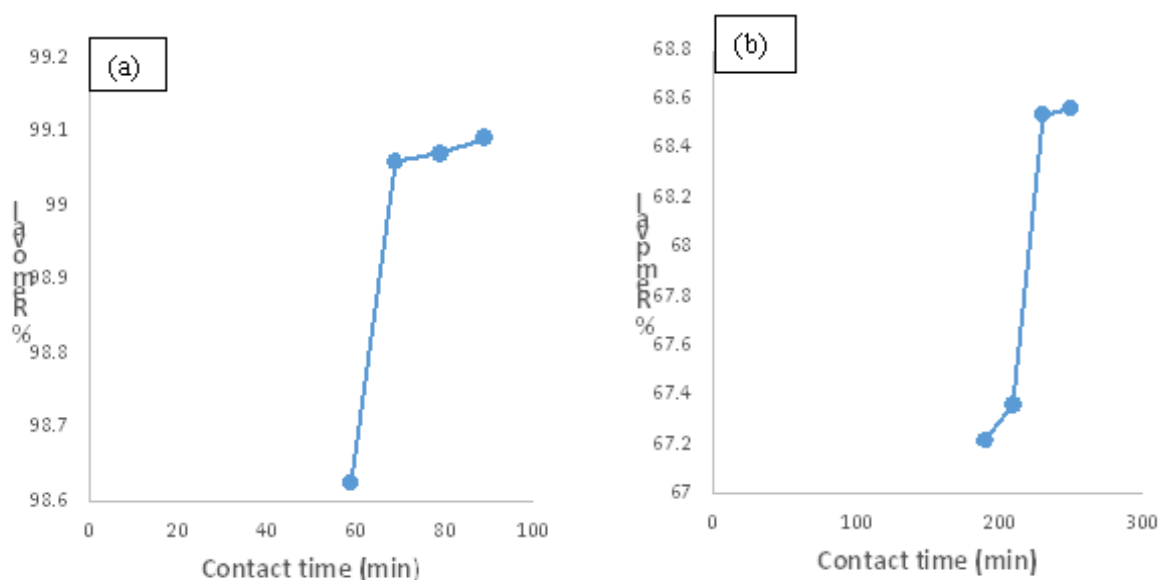


Figure.3: Effect of contact time on adsorption of (a)BG dye, and (b) AA27 onto AZ

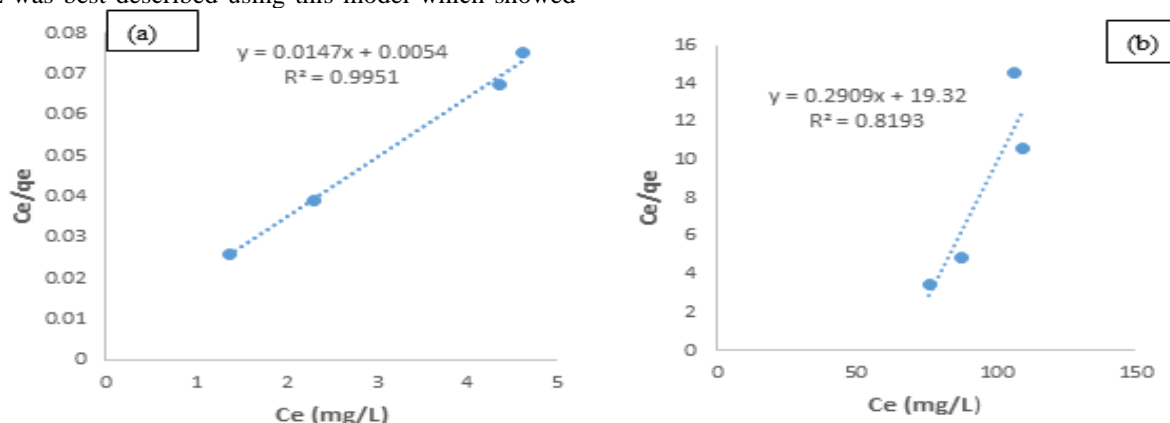
### 3.5 Adsorption isotherm

Fig. 8a and 8b represented the Langmuir isotherm plots of BG and AA27 respectively. Table 9 shows the adsorption

parameters in the adsorption on activated LAU-NZ, along with the correlation coefficient  $R^2$  of nearly 1. In Fig 8, the maximum adsorption capacities ( $q_{max}$ ) of the AZ were

found to be 68.02 mg/g, and 3.43 mg/g for BG and AA27. Therefore, the adsorption of BG on activated LAU-NZ was best described using this model which showed

single monolayer adsorption of BG on the surface of activated LAU-NZ as compared to AA27.



**Figure4: Langmuir isotherm plots of (a) BG and (b) AA27 27 onto AZ**

The Freundlich isotherm shows the plot of  $\log C_e$  vs.  $\log q_e$  as shown in Fig. 9a for BG and Fig.9b for AA27, respectively and both the values of  $1/n$  and  $K_f$  can be calculated from the slope and intercept. It is considered good adsorption if the  $n$  value is ( $0 > n < 1$ ) (Munagapati *et al.*, 2021). In this study, the  $n$  value obtained from

Freundlich model for BG and AA 27 was found to be 10.47 and 0.37, respectively, indicating the adsorption of BG is unfavorable and that of AA27 is favorable. This indicate that this isotherm is a better representation model for Acid red 27 dye.

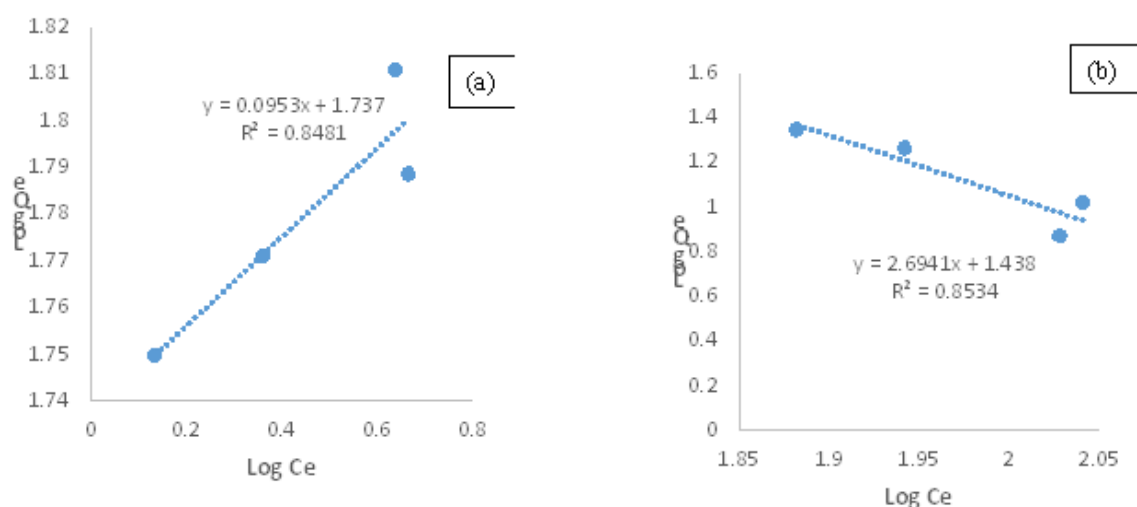


**Figure 5: Freundlich isotherm plots of (a) BG, and (b) AA27 onto AZ**

**Table 9: The adsorption isotherms parameters for Langmuir and Freundlich model**

Adsorption parameters	Brilliant Green	Acid Red 27
<b>Langmuir isotherm</b>		
$K_L$ (L/mg)	2.72	5.62
$q_{max}$ (mg/g)	68.02	3.43
$R^2$	0.9951	0.8193
$R_L$	0.0017	0.0015

Adsorption parameters	Brilliant Green	Acid Red 27
<b>Langmuir isotherm</b>		
<b>Freundlich isotherm</b>		
$K_f$ (mg/g)	54.58	27.42
$1/n$	0.0953	2.6941
$R^2$	0.8421	0.8534

#### 4. CONCLUSION

The removal efficiency and maximum adsorption capacities of BG and AA27 were 68.02 and 3.43 mg/g respectively with optimum removal efficacy of 96.24% and 83.14%. Characterization on the LAU-NZ by SEM, XRD and XRF. FTIR analysis was done on the activated and after adsorption. The optimal experimental conditions for the removal of the maximum dye were determined on contact time, initial concentration, and adsorbent dosage. From ANOVA, it showed that the BBD model was statically significant. It was observed that the independent variables were all significant which implies that all factors variable studied had specific impact on its removal efficiency. Numerical optimization (unity) was found to be the desirability values of these parameters, which represent the ideal and desired values. Isotherms models of Langmuir and Freundlich were applied to study adsorption of BG and AA27 on activated natural zeolite. The adsorption behavior of Langmuir was best represented ( $R^2 = 0.9951$ ) for BG with maximum adsorption capacity of 68.02 mg/L and AA27 is described by Freundlich isotherm ( $R^2 = 0.8534$ ). The current investigation reveals that the activated Laumontite zeolite that has been made using inexpensive method was effectively used in the removal Acid Red 27 and Brilliant Green, from simulated dye wastewater that and the results prove very successful.

#### ACKNOWLEDGMENT

This research was funded with the support of TETFUND National Research Fund with grant number TETF/ES/DR&D-CE/NRF2023/SETI/ARS/0039/VOL-1.

#### REFERENCES

- Albadarin, A. B., Collins, M. N., Naushad, M., Shirazian, S., Walker, G., & Mangwandi, C. (2017). Activated lignin-chitosan extruded blends for efficient adsorption of methylene blue. *Chemical Engineering Journal*, 307, 264–272. <https://doi.org/10.1016/j.cej.2016.08.089>
- Alakhras, F., Alhajri, E., Haounati, R., Ouachtak, H., Addi, A. A., & Saleh, T. A. (2020). A comparative study of photocatalytic degradation of Rhodamine B using natural-based zeolite composites. *Surfaces and Interfaces*, 20(May). <https://doi.org/10.1016/j.surfin.2020.100611>
- Alene, A. N., Abate, G. Y., & Habte, A. T. (2020). Bioadsorption of Basic Blue Dye from Aqueous Solution onto Raw and Modified Waste Ash as Economical Alternative Bioadsorbent. *Journal of Chemistry*, 2020. <https://doi.org/10.1155/2020/8746035>
- Bader, A., Hartwich, M., Richter, A., & Meyer, B. (2018). Numerical and experimental study of heavy oil gasification in an entrained-flow reactor and the impact of the burner concept. *Fuel Processing Technology*, 169(September 2017), 58–70. <https://doi.org/10.1016/j.fuproc.2017.09.003>
- Bushra, R., Mohamad, S., Alias, Y., Jin, Y., & Ahmad, M. (2021). Current approaches and methodologies to explore the perceptive adsorption mechanism of dyes on low-cost agricultural waste: A review. *Microporous and Mesoporous Materials*, 319(December 2020), 111040. <https://doi.org/10.1016/j.micromeso.2021.111040>
- Cui, C., Chen, A., Pan, Z., & Ma, R. (2019). Two-dimensional numerical model and fast estimation method for calculating crevice corrosion of cross-sea bridges. *Construction and Building Materials*, 206, 683–693. <https://doi.org/10.1016/j.conbuildmat.2019.02.103>
- Hasan, F. (2023). *Synthesis Of Zeolite Granules From NaCl Activated- Nano Zeolite Ore To Remove Calcium Ions From Groundwater*. 0–14.
- Lau, W. J., & Ismail, A. F. (2009). Polymeric nanofiltration membranes for textile dye wastewater treatment: Preparation, performance evaluation, transport modelling, and fouling control - a review. *Desalination*, 245(1–3), 321–348. <https://doi.org/10.1016/j.desal.2007.12.058>
- Hosaka, H., Itao, K., & Kuroda, S. (1995). Damping characteristics of beam-shaped micro-oscillators. In *"Sensors and Actuators, A: Physical"* (Vol. 49, Issues 1–2, pp. 87–95). [https://doi.org/10.1016/0924-4247\(95\)01003-J](https://doi.org/10.1016/0924-4247(95)01003-J)
- Jahan, R. A., Hassan, M., Rana, A. A., & Karim, M. M. (2023). *Adsorption of Anionic and Cationic Dyes from Textile Effluents by Activated Carbon Prepared from Sawdust and Fish Scale*. 189–202. <https://doi.org/10.4236/aces.2023.133014>
- Kumar, B. V. S. (2019). *Characterization of zeolites by infrared spectroscopy*. August.
- Mahmoud, A. S., Farag, R. S., & Elshfai, M. M. (2020). Reduction of organic matter from municipal wastewater at low cost using green synthesis nano iron extracted from black tea: Artificial intelligence with regression analysis. *Egyptian Journal of Petroleum*, 29(1), 9–20. <https://doi.org/10.1016/j.ejpe.2019.09.001>
- Mansour, R. A., Shahawy, A. El, Attia, A., & Beheary, M. S. (2020). *Brilliant Green Dye Biosorption Using Activated Carbon Derived from Guava Tree Wood*. 2020.
- Munagapati, V. S., Wen, H., Vijaya, Y., Wen, J., Tian, Z., Reddy, G. M., & Raul, J. (2021). Removal of anionic ( Acid Yellow 17 and Amaranth ) dyes using aminated avocado ( Persea americana ) seed powder : adsorption / desorption , kinetics , isotherms , thermodynamics , and recycling studies. *International Journal of Phytoremediation*, 0(0), 1–13. <https://doi.org/10.1080/15226514.2020.1866491>
- Pathania, D., Gupta, D., Al-Muhtaseb, A. H., Sharma,

- G., Kumar, A., Naushad, M., Ahamad, T., & Alshehri, S. M. (2016). Photocatalytic degradation of highly toxic dyes using chitosan-g-poly(acrylamide)/ZnS in presence of solar irradiation. *Journal of Photochemistry and Photobiology A: Chemistry*, 329, 61–68. <https://doi.org/10.1016/j.jphotochem.2016.06.019>
- Rahaman, A., Rashed, M. A., Rahaman, M. A., Tozammel, M., & Sumon, H. (2022). A comparative study of the adsorptive removal of toxic amaranth dye from aqueous solution using low cost bio-adsorbents. *International Journal of Chemical Studies*, 10(1).
- Samaka, I. A. S. (2021). Using Agricultural Waste as Biosorbent for Hazardous Brilliant Green Dye Removal from Aqueous Solutions. 16(4), 3435–3454.
- Santos, S. C. R., & Boaventura, R. A. R. (2015). Treatment of a simulated textile wastewater in a sequencing batch reactor (SBR) with addition of a low-cost adsorbent. *Journal of Hazardous Materials*, 291, 74–82. <https://doi.org/10.1016/j.jhazmat.2015.02.074>
- Soscún, H., Castellano, O., Hernández, J., & Hinchliffe, A. (2001). Acidity of the Brönsted acid sites of zeolites. *International Journal of Quantum Chemistry*, 82(3), 143–150. [https://doi.org/10.1002/1097-461X\(2001\)82:3<143::AID-QUA1014>3.0.CO;2-Q](https://doi.org/10.1002/1097-461X(2001)82:3<143::AID-QUA1014>3.0.CO;2-Q)
- Tounsadi, H., Khalidi, A., Machrouhi, A., Farnane, M., Elmoubarki, R., Elhalil, A., Sadiq, M., & Barka, N. (2016). Highly efficient activated carbon from *Glebionis coronaria* L. biomass: Optimization of preparation conditions and heavy metals removal using experimental design approach. *Journal of Environmental Chemical Engineering*, 4(4), 4549–4564. <https://doi.org/10.1016/j.jece.2016.10.020>
- Treacy, M. M., & Higgins, J. B. (2007). *Collection of simulated XRD powder patterns for zeolites fifth (5th) revised edition*. Elsevier.
- Wu, J., Wang, G., Li, Z., Yu, E., Xie, J., & Zheng, Z. (2017). Extraction of flocculants from a strain of *Bacillus thuringiensis* and analysis of their properties. *Aquaculture and Fisheries*, 2(4), 179–184. <https://doi.org/10.1016/j.aaf.2017.06.003>
- Zafar, M. N., Ghafoor, S., Tabassum, M., Zubair, M., Nazar, M. F., & Ashfaq, M. (2020). Utilization of peanut (*Arachis hypogaea*) hull based activated carbon for the removal of amaranth dye from aqueous solutions. *Iranian Journal of Chemistry and Chemical Engineering*, 39(4), 183–191. <https://doi.org/10.30492/ijcce.2019.34951>

**JOURNAL OF THE NIGERIAN SOCIETY  
OF CHEMICAL ENGINEERS  
INSTRUCTION TO AUTHORS**

**1. TYPES OF PUBLICATION**

The Journal of the Nigerian Society of Chemical Engineers will publish articles on the original research on the science and technology of Chemical Engineering. Preference will be given to articles on new processes or innovative adaptation of existing processes. Critical reviews on current topics of Chemical Engineering are encouraged and may be solicited by the Editorial Board. The following types of articles will be considered for publication:

- a. Full length **articles or review papers**.
- b. **Communication** – a preliminary report on research findings.
- c. **Note** – a short paper describing a research finding not sufficiently completed to warrant a full article.
- d. **Letter to the Editor** – comments or remarks by readers and/or authors on previously published materials.

The authors are entirely responsible for the accuracy of data and statements. It is also the responsibility of authors to seek ethical clearance and written permission from persons or agencies concerned, whenever copyrighted material is used.

For now the journal is published twice in a year, March/April and September/October.

**2. MANUSCRIPT REQUIREMENTS**

- a. The **Manuscript** should be written in clear and concise English and typed (single column) in Microsoft Word using double spacing on A4-size paper, Times New Romans font and 12 point. A full length article or review should not exceed 15 pages. Margin should be Normal (i.e. 2.54cm for Top, Bottom, Left & Right margins).
- b. The **Manuscript** should be prepared in the following format: Abstract, Introduction, Materials and Methods, Results, Discussion, Conclusion, Acknowledgements, and References..
- c. The **Manuscript** must contain the full names, address and emails of the authors. In the case of multiple authorship, the person to whom correspondence should be addressed must be indicated with functional email address. As an examples, authors' names should be in this format: **Momoh, S. O., Adisa, A. A. and Abubakar, A. S.** If the addresses of authors are different, use the following format:

**\*Momoh, S. O.<sup>1</sup>, Adisa, A. A.<sup>2</sup> and Abubakar, A. S.<sup>3</sup>**

Use star \* to indicate the corresponding author.

- d. **Symbols** should conform to America Standard Association. An abridged set of acceptable symbols is available in the fourth edition of Perry's Chemical Engineering Handbook. Greek letters, subscripts and superscripts should be carefully typed. A list of all symbols used in the paper should be included after the main text as **Nomenclature**.
- e. All **Units** must be in the SI units (kg, m, s, N, etc).
- f. The **Abstract** should be in English and should not be more than 200 words. The Abstract should state briefly the purpose of the research, methodology, results, major findings and major conclusions. Abstracts are not required for Communications, Notes or Letters.
- g. **Citation** must be in the Harvard Format i.e. (Author, Date). Examples are (Smith, 1990) or (Jones et al, 2011). (Kemp, 2000) demonstrated that .....; (Mbuk, 1985; Boma, 1999; Sani, 2000) if more than two authors. (Telma, 2001a), (Telma, 2001b); etc if the citation have the same author and year of publication. For more information on Harvard Referencing: Guide visit <http://www.citethisforme.com/harvard-referencing>
- h. **References** must also be in the Harvard Format i.e. (Author, Date, Title, Publication Information). References are listed in alphabetical order. Examples are shown below:  
Haghi, A. K. and Ghanadzadeh, H. (2005). A Study of Thermal Drying Process. *Indian Journal of Chemical Technology*, Vol. 12, November 2005, pp. 654-663  
Kemp, I.C., Fyhr, C. B., Laurent, S., Roques, M. A., Groenewold, C. E., Tsotsas, E., Sereno, A. A., Bonazzi, C. B., Bimbernet, J. J. and Kind M.(2001). Methods for Processing Experimental Drying Kinetic Data. *Drying Technology*, 19: 15-34.
- i. **Tables** should contain a minimum of descriptive materials. Tables should be numbered serially throughout the manuscript in Arabic numerals (1, 2, 3, etc), and should be placed at the referenced point with captions (centralised) placed at the top of the table.
- j. **Figures**, charts, graphs and all illustrations should be placed at the referenced point, numbered serially throughout the manuscript in Arabic numerals (1, 2, 3, etc) and incorporated in the text. Caption for

Figures should be placed at the bottom of the Figure (centralised). Lettering set or symbols should be used for all labels on the figures, graphs, charts, photographs even when drawn in colours. (Note that figures drawn in colours may be unreadable if printed in black and white).

- k. **Equations** should be typed using MS Word Equation Editor and should be centred and numbered serially throughout the manuscript (in Arabic numeral) at the right margin.
- l. Wherever possible, **Fractions** should be shown using the oblique slash. E.g. x/y
- m. **Footnotes** should not be incorporated in the text.
- n. **Acknowledgements** should appear at the end of the paper, before the list of references.

### 3. SUBMISSION OF MANUSCRIPTS

Manuscripts should be submitted by sending a Microsoft Word document (taking into account the Manuscript Requirements described in section 2 above) to the following email address: [nschejournal@yahoo.com](mailto:nschejournal@yahoo.com) and copy [stevmomoh@yahoo.com](mailto:stevmomoh@yahoo.com).

All correspondences are directed to the Editor-in-Chief using the submission emails addresses: [nschejournal@yahoo.com](mailto:nschejournal@yahoo.com) and copy [stevmomoh@yahoo.com](mailto:stevmomoh@yahoo.com). Meanwhile the online submission of articles on the journal website will soon be ready.

Authors should note that:

- a. All authors listed in the manuscript have significantly contributed to the research.
- b. All authors are obliged to provide retractions or corrections of mistakes.
- c. All references cited are listed and financial support acknowledged.
- d. It is forbidden to publish same research in more than one journal.

The fee charged for paper review and publication will be borne by the authors as follows:

- a. Manuscript Review charges = N6,500 payable by both Members and Non-Member. Overseas is \$30.00.
- b. Publication Charges = N10,000 payable by Non-Members and Members who are not financially up-to-date. Overseas is \$40.00.
- c. Members would only get one (1) Journal free and buy the other if they so wish.
- d. Corresponding Author whose paper is published on a particular edition would get one (1) free copy on behalf of all the co-authors. Other co-authors will buy if they so wish.

All fees are paid after the paper had been accepted for publication. These charges may be reviewed from time to time by the Governing Board of Directors of the Society.

### 4. ACCEPTED PAPERS

On acceptance, authors will be required to submit a copy of their manuscripts using Microsoft Word by emails to [nschejournal@yahoo.com](mailto:nschejournal@yahoo.com) and copy [stevmomoh@yahoo.com](mailto:stevmomoh@yahoo.com).

The following additional information should be observed for accepted papers: (i) Typed in Microsoft Word using 1.15 spacing on A4-size paper, Times New Romans font and 10 point; (ii) Margin should be 2.54cm for Top & Bottom; 2.20cm for Left & Right margins; (iii) The abstract should be one column document while the body of the manuscript should be double columns with 0.5cm gutter spacing except some tables and figures that may have to go in for one column document.

### 5. PUBLICATION

Full NSChE Journal edition in hard copy will be published twice annually – March/April Edition and September/October Edition.

### 6. REPRINT

Reprints are available on request at a moderate fee per page. Orders must be placed before the paper appears in Print.

### 7. READER'S INFORMATION

The papers are wholly the view of their author(s) and therefore the publisher and the editors bear no responsibility for such views.

### 8. SUBSCRIPTION INFORMATION

The subscription price per volume is as follows:

- a. Individual Reader - N3,000.00
- b. Institutions, Libraries, etc.- N5,000.00
- c. Overseas Subscription - \$100.00

Request for information or subscription should be sent to the Editor-in-Chief through the following emails addresses: [nschejournal@yahoo.com](mailto:nschejournal@yahoo.com) and copy [stevmomoh@yahoo.com](mailto:stevmomoh@yahoo.com).

### 9. COPYRIGHT NOTICE

By submitting your manuscript to the Journal, you have agreed that the copyright of the published material belongs to the journal.

### 10. PRIVACY STATEMENT

The names and email addresses entered in this journal site will be used exclusively for the stated purposes of this journal and will not be made available for any other purpose or to any other party.

## **THE PUBLICATION CHARGES**

1. The publication charges totaling Sixteen Thousand Five Hundred Naira (₦16,500) only shall be payable to the following account per an article.

**Name of account: Nigerian Society of Chemical Engineers**

**UBA account No:1001730178**

**or**

**GTB account No 0139519728**

2. The narration on the slip should be “**Journal Publication Charges**”
3. Make your payments and send a proof to the email of the Chairman/Editor-in-Chief, [stevmomoh@yahoo.com](mailto:stevmomoh@yahoo.com) at a specified date





***Providing Continuous Value  
and Quality Products & Services  
For our Esteemed Customers***



**OIL & GAS SERVICES**

**Chemical Services  
Pipeline Services**

**LUBRICANTS &  
PETROLEUM PRODUCTS**

**MATRIX PETRO-CHEM LIMITED**

**1, Wilmer Street,**

**Off Town Planning Way, Ilupeju,**

**P.O. Box 5652, Ikeja, Lagos, Nigeria.**

**Tel: 01-4936873, 4822948, Fax: 01-4936873**

**info@matrixpetrochem.com**

**PORT-HACOURT**

**Plot 3c, Trans Amadi,**

**Rumuobiokani,**

**Port-Hacourt.**

**084-794615**